Title: Intestinal Bacteria are Necessary for Doxorubicin-induced Intestinal Damage but not for Doxorubicin-induced Apoptosis.

Running Title: Doxorubicin-induced damage dependent on intestinal bacteria

Authors: Rachael J. Rigby[1], Jacquelyn Carr[2], Kelly Orgel[3,4], Stephanie L. King[5], P. Kay Lund[4], and Christopher M. Dekaney[2,5]

Affiliations: [1]Faculty of Health and Medicine, Lancaster University, Lancaster, United Kingdom; Departments of [2]Surgery, [3]Pediatrics and [4]Cell Biology and Physiology, The University of North Carolina, Chapel Hill, North Carolina; [5]Department of Molecular Biomedical Sciences, North Carolina State University, Raleigh, North Carolina

Contact information:

Christopher M. Dekaney, Ph.D.
North Carolina State University
1060 William Moore Drive
Raleigh, North Carolina 27607-8401
Phone: 919-513-6372
Email: chris_dekaney@ncsu.edu

Keywords: intestine, bacteria, doxorubicin, germ free, damage, apoptosis

Abbreviations: Doxorubicin (DOXO), intestinal epithelial cell (IEC), conventionalized (CONV), germ free (GF), intraperitoneal (IP), hematoxylin and eosin (H&E)

Abstract

Doxorubicin (DOXO) induces significant, but transient, increases in apoptosis in the stem cell zone of the jejunum, followed by mucosal damage involving a decrease in crypt proliferation, crypt number, and villus height. The gastrointestinal tract is home to a vast population of commensal bacteria and numerous studies have demonstrated a symbiotic relationship between intestinal bacteria and intestinal epithelial cells (IEC) in maintaining homeostatic functions of the intestine. However, whether enteric bacteria play a role in DOXO-induced damage is not well understood. We hypothesized that enteric bacteria are necessary for induction of apoptosis and damage associated with DOXO treatment**.** Conventionally raised (CONV) and germ free (GF) mice were given a single injection of DOXO, and intestinal tissue was collected at 6, 72, and 120 h after treatment and from no treatment (0 h) controls. Histology and morphometric analyses quantified apoptosis, mitosis, crypt depth, villus height, and crypt density. Immunostaining for muc2 and lysozyme evaluated Paneth cells, goblet cells or dual stained intermediate cells. DOXO administration induced significant increases in apoptosis in jejunal epithelium regardless of the presence of enteric bacteria; however, the resulting injury, as demonstrated by statistically significant changes in crypt depth, crypt number, and proliferative cell number, was dependent upon the presence of enteric bacteria. Furthermore, we observed expansion of Paneth and goblet cells and presence of intermediate cells only in CONV and not GF mice. These findings provide evidence that manipulation and/or depletion of the enteric microbiota may have clinical significance in limiting chemotherapy-induced mucositis.

Introduction

The small intestinal epithelium is one of the most rapidly proliferating tissues in the body. This property renders intestinal epithelial cells (IEC) particularly susceptible to chemotherapy-induced damage which is reported in up to 40% of patients who receive chemotherapy. [1] Chemotherapy-induced cytotoxicity within the gastrointestinal tract manifests as mucositis, characterized by gross ulcerations of the intestinal mucosa. The development of mucositis is a limiting factor in administration of chemotherapeutic agents, and therefore strategies to reduce this side-effect are urgently sought.

Doxorubicin (DOXO) is a common chemotherapeutic utilized for sarcomas, select breast cancers, and several metastatic cancers. We previously reported that a single injection of DOXO given to mice induced significant, but transient, increases in apoptosis in the stem cell zone of the jejunum, followed by mucosal damage involving a decrease in crypt proliferation, crypt number, and villus height. [2] Subsequently, repair occurred, characterized by crypt hypertrophy, Paneth cell hyperplasia and, ultimately, return of the intestinal mucosa to normal morphology. [3]

The gastrointestinal tract is home to a vast population of commensal bacteria and numerous studies have demonstrated the importance of the symbiotic relationship between intestinal bacteria and IECs in maintaining homeostatic functions of the intestine, including nutrient generation and metabolism and proper development of the innate immune system. [4,5,6,7] Evidence in models of intestinal damage, indicate distinct effects of bacteria in different regions of the gastrointestinal tract. For example, in colon of mice that lack TLR signaling (MyD88-/-), restitution and repair following epithelial injury is impaired. [8] Similarly, germ free (GF) mice have shorter colonic crypts [9] and are more susceptible to chemical-induced injury, [10] providing additional support for a role of commensal microbiota in sustaining epithelial integrity or promoting mucosal repair in the colon. In contrast, in the small intestine, the

presence of enteric bacteria and/or bacterial products appears to exacerbate damage. For example, in both TLR4-/- and MyD88-/- mice, intestinal damage after exposure to indomethacin was abrogated. [11] Similarly, deficiency of TLR2 or TLR9 expression or inhibition of TLR9 activity were associated with significantly decreased DOXO-induced damage to the small intestine. [12] Additionally, the microbiota promotes inflammation and fibrosis following small bowel resection, [13] reflective of the 'double edged-sword' role of intestinal microbiota associated-signaling in mucosal repair. These data led us to question whether enteric bacteria play a role in mucosal damage associated with chemotherapeutic agents like DOXO.

In this report, we tested the hypothesis that enteric bacteria were necessary for induction of apoptosis and mucosal damage associated with DOXO treatment. Our data show that DOXO administration induces apoptosis regardless of the presence of enteric bacteria, but that the resulting damage, as demonstrated by changes in crypt depth, crypt number, and proliferative index, is enteric bacteria-dependent. These findings provide evidence that manipulation and/or depletion of the enteric microbiota may have clinical significance in limiting chemotherapy-induced mucositis.

Results

DOXO treatment rapidly induced apoptosis in both GF and CONV small intestine.

We previously reported that DOXO exposure rapidly induces apoptosis in crypt epithelium of CONV mice and that apoptosis peaked at 6h and remained elevated relative to control mice out to 120h after DOXO treatment. [2] In the current study, similar levels of apoptosis were observed in crypt epithelium of both GF and CONV mice, as assessed by both H&E staining and cleaved caspase 3 (Fig. 1A), at 6h following DOXO treatment. However, by 72h post DOXO treatment apoptosis had returned to baseline levels (Fig. 1B). Consistent with prior findings [2] cell positional analysis revealed that DOXO-induced apoptosis occurred primarily in cell positions 3-6, indicative of involvement of the intestinal stem cell zone (Fig. 1C). Although not significantly different from CONV, there may be an indication that apoptosis is occurring in cell positions higher up the crypt in GF, compared with CONV mice. This may suggest that cells of different lineages and/or differentiation status are more susceptible to DOXO-induced apoptosis in GF vs. CONV mice, or that DOXO-induced apoptosis induces a higher turnover in GF mice.

Alterations in villus-crypt morphometry in CONV, but not GF mice, following DOXO.

We previously demonstrated that an increase in crypt depth 120h following DOXO treatment was a hallmark of the repair phase and that villus blunting was evident at that time as well. [2] Though GF crypts were significantly shorter than CONV crypts at baseline, GF mice showed no significant change in crypt depth throughout the entire time course after DOXO treatment (Fig. 2A and B). In contrast, by 120h after DOXO, crypts were significantly deeper in CONV mice compared to both control CONV mice and to GF mice at 120h after DOXO. GF mice showed no significant change in villus height throughout the entire time course after DOXO treatment (Fig. 2C). CONV mice, while not statistically different, demonstrated a trend toward shorter villi after DOXO treatment similar to our previous report. [2]

Our previous studies demonstrated a significant increase in proliferative index during repair following DOXO-induced damage which marked the movement of the intestinal mucosa in the repair phase. [2] Immunohistochemistry revealed a significant increase in the number $pHH3^{+}$ cells in crypt epithelium of CONV mice at 120h following DOXO treatment, indicating an increase in crypt cell proliferation and this increase was not observed in GF mice (Fig. 3A and B). Similarly, we previously observed increases in the number of mitotic figures in crypt epithelium during repair. [2] Evaluation of the number of mitotic figures per crypt in both GF and CONV mice following DOXO revealed significantly decreased numbers in both GF and CONV crypts at 6h following DOXO, consistent with induction of DNA damage and cell cycle arrest (Fig. 3C). The number of mitotic figures per crypt remained significantly decreased in CONV mice but returned to control levels in GF mice at 72h following DOXO. A return of mitotic figure number to control levels in CONV mice was observed by 120h following DOXO treatment. Of note, at baseline the number of mitotic figures per crypt was significantly greater in CONV compared to GF mice.

We previously demonstrated that DOXO-treatment of CONV mice resulted in significant crypt loss by 72h and this loss of crypts can be used as an indicator of loss of intestinal stem cells. [2] Although apoptosis and cell cycle arrest were observed in both GF and CONV crypt epithelium following DOXO treatment, only in CONV mice was this followed by significant loss of crypt number assessed by reduced crypt density. By 72h following DOXO treatment, crypt density was significantly decreased in CONV mice compared to control CONV mice, and compared to GF mice at 72h after treatment with DOXO (Fig. 4). This decrease in crypt density was still observed at 120 h after DOXO in CONV mice, but trended toward restitution of crypt number similar to our previous findings. [2]

Expansion of the Paneth cell compartment is absent in GF mice following DOXO treatment.

We previously reported an expansion of the Paneth cell compartment in jejunal crypts following DOXO-induced damage in CONV mice which in turn increases the intestinal stem cell niche. [2] This expansion included an increase in total lysozyme-positive cell and intermediate cell (muc2 and lysozyme expressing cell) numbers suggesting alteration in secretory cell lineage allocation or maturation. [3] As Paneth cells play a critical role in sensing and responding to enteric bacteria [14] we wished to evaluated whether the absence of enteric bacteria in GF mice would alter the Paneth cell compartment. Following DOXO treatment, staining sections for lysozyme and muc2 revealed an expansion of lysozyme-positive cells at the crypt base 120 h after DOXO in CONV mice. In addition, staining revealed the presence of muc2- and lysozyme-expressing intermediate cells in CONV mice following DOXO treatment (Fig. 5). This is in contrast to the lack of expansion of lysozyme-positive cell numbers and presence of intermediate cells is observed in GF crypts following DOXO treatment (Fig. 5).

Discussion

This study demonstrates that enteric bacteria are necessary for the initiation and maintenance of mucosal damage and repair observed in the jejunum of CONV mice following DOXO treatment, which includes crypt loss and villus blunting, followed by an increase in proliferating cells, and crypt hyperplasia. In contrast, enteric bacteria do not appear to be necessary for the rapid DOXO-mediated induction of apoptosis which was induced to similar levels in both GF and CONV raised mice, and in a similar cell position distribution. Likewise, DOXO treatment results in a decreased number of mitotic figures in the crypt epithelium of both GF and CONV mice. Together, these data suggest that the damage-associated crypt loss and subsequent crypt regeneration documented in CONV mice is *not* secondary to the rapid induction of apoptosis observed in crypt epithelial cells following DOXO treatment; but, rather, is coupled to the presence of enteric bacteria. While DOXO is a widely used anticancer drug, its mechanism of action is not completely understood. Classically, DOXO is described as a topoisomerase II inhibitor and, as such, inhibits the re-ligation of cleaved DNA strands which have been unwound for transcription and replication. This inhibition results in DNA double strand breaks, and ultimately, apoptosis of the cell. [15] Other mechanisms of induction of apoptosis by DOXO have been suggested, as well, including inhibition of DNA and RNA synthesis and formation of free radicals or formaldehyde-mediated DOXO-DNA adducts. [16] Nonetheless, regardless of the mechanism of action of DOXO within the small intestinal epithelium, our data demonstrate that DOXO induces apoptosis *independent of* the presence of enteric bacteria. What is unclear are the events that occur after the initial induction of apoptosis, which culminate in crypt loss, villus shrinking, crypt hyperplasia, and subsequent restitution of normal small intestinal mucosa, and moreover, what specific roles enteric bacteria play in this damage and repair process.

One possibility is that DOXO treatment elicits a direct effect upon intestinal bacteria, causing a rapid dysbiosis which, in turn, causes direct damage to the intestinal epithelium, as has been shown for methotrexate. [17] A similar theory has been put forth for the role of dysbiosis in susceptibility for inflammatory bowel disease. [18,19] Though it is used in human medicine primarily for its antineoplastic properties, DOXO is a natural anthracycline antibiotic product of *Streptomyces peucetius* var. *casieus.* [20] Since DOXO targets rapidly dividing cells, and bacteria tend to replicate frequently, bacteria may, indeed, be potential primary targets. Interestingly, studies suggest that unconjugated DOXO may be available to small intestinal enteric bacteria within a few hours after dosing. [21] These studies were performed on isolated perfused rat liver, and showed that approximately 30% of a dose of DOXO (equivalent to a 20 mg/kg intravenous dose) was excreted from isolated liver as unconjugated DOXO into bile within 3 h of dosing. [21] However, *in vitro* studies indicate that DOXO has little direct impact on bacterial growth. These prior findings provide no evidence that DOXO induces a dysbiosis of the enteric bacterial census, however they do not inform about potential effects on specific bacteria. Also, our findings do not rule out the possibility that dysbiosis occurs following DOXO-induced damage by an indirect, but DOXO-dependent, mechanism. Other chemotherapeutic drugs have been shown to be reactivated by microbial β-glucuronidases, leading to direct toxicity to mucosal cells. [22,23,24] Therefore, further studies to evaluate microbial-dependent mucositis following DOXO treatment are underway.

Another potential mechanism of enteric bacteria-mediated intestinal damage following DOXO treatment is disruption of the physical barrier that separates the intestinal epithelium from luminal bacteria. In healthy intestine under homeostatic conditions, a barrier of mucin serves to minimize the direct contact of luminal bacteria with the mucosa. [25] In addition, Paneth cells secrete a cadre of antimicrobial factors including: a-defensins, aPLA2, and lysozyme. [26] However, DOXO-may alter barrier function, permitting an increase in the direct

association of bacteria with the epithelium, followed by initiation of a bacteria-dependent signaling cascade via TLR or NOD receptors. An absence of bacteria, therefore, would fail to trigger this cascade. Of note, Nigro et al. demonstrated an increase in DOXO-induced apoptosis and dampened repair in Nod2 knock out mice suggesting that the presence of bacterial products such as muramyl-dipeptide (MDP) might be protective during damage. [27] However, because Nod2 was knocked out in the entire mouse it is not clear whether the protective effect came from Nod2 signaling within intestinal epithelium or lamina propria-derived cells. Other pro-mucositis chemotherapeutic agents, such as irinotecan, have been shown to impact mucin secretion, [28] and closer association of microbes with mucosa offers increased opportunities for activation of TLR and/or NODs on or within epithelial cells and immune cells intimately associated with the epithelial barrier. [29,30] Likewise, our previous studies demonstrate alteration in secretory cell allocation within the intestinal crypt, resulting in increased intermediate cell (both muc2 and lysozyme positive) number which may alter the mucin barrier. [2,3] This finding is echoed by the increase in muc2^{+}/lysozyme^{+} cells observed in crypts of CONV mice at five days after DOXO in the current study. The fact that increases in muc2^{+}/lysozyme^{+} cells were not observed in GF mice after DOXO treatment may reflect an absence of damage and regenerative response or indicate that the alterations in lineage allocation that follow DOXO result from an increased interaction between enteric bacteria and epithelium.

Alternatively, DOXO-driven disruption of the mucosal barrier may not increase the association between bacteria and epithelia, but instead allow direct penetration of bacteria or bacterial products through a more permeable epithelium and into the lamina propria, facilitating direct interaction with resident leukocytes. Sun et al. demonstrated an increase in epithelial permeability of rat small intestinal epithelium following treatment with DOXO. [31] This increase allowed particles as large as albumin to move from the intestinal lumen to the lamina

propria, suggesting that an increase in permeability following DOXO may allow bacteria and/or bacterial products to penetrate the IEC barrier. DOXO treatment may also result in an inflammatory response following penetration of the epithelial barrier by bacterial products, or via another distinct pathway, such as the AKT-dependent inflammation that leads to cardiomyopathy following DOXO, or the CCL2-dependent inflammation that leads to renal fibrosis following DOXO. [32,33] To elucidate these mechanisms, future investigations will evaluate epithelial permeability, as well as the role of the inflammatory response, following DOXO. We hypothesize that treatment with DOXO causes an increase in the permeability of the epithelial barrier (due to a transient induction of increased apoptosis), concomitant with increased association of enteric bacteria with the mucosa, allowing bacterial products to penetrate and induce an inflammatory response, resulting in the significant mucosal damage (and repair) observed in our studies.

The findings of the current study demonstrate that DOXO-induced apoptosis in small intestinal crypts occurs independent of the presence of bacteria while mucosal damage after DOXO is dependent upon the presence of bacteria. These findings have translational implications supporting that manipulation of the intestinal microbiota during DOXO-based chemotherapy may reduce damage to the intestinal mucosa. This could allow more effective anticancer therapies with fewer adverse effects

Materials and Methods

Animals. Conventionally raised (CONV) adult female C57BL/6 mice were purchased from Jackson Laboratories and used between 8-10 weeks of age. Adult female C57BL/6 mice were raised under germ free (GF) conditions in the National Gnotobiotic Research Center at the University of North Carolina at Chapel Hill. Experimental procedures were approved by the Institutional Animal Care and Use Committee of The University of North Carolina at Chapel Hill. Mice were given a single intraperitoneal (IP) injection of DOXO (Pharmacia & Upjohn Co.) at a dose of 20 mg/kg body weight. We have previously reported that this dose induces a reproducible sequela of intestinal damage in mice. [2] Animals were killed at 6 (n=3 for CONV, n=3 for GF), 72 (n=3, n=3), or 120 h (n=3, n=2) after DOXO treatment and compared with no treatment controls (n=3, n=6). Small intestine was flushed with ice-cold phosphate buffered saline (pH 7.4) and a piece of middle jejunum was fixed in 10% buffered formalin and embedded in paraffin.

Histology. Formalin-fixed paraffin embedded specimens were oriented to provide sections perpendicular to the long axis of the bowel, and 5μm sections were used for evaluating general morphology. Longitudinal sections of crypts or villi were selected for scoring on the basis that a single, continuous layer of epithelium followed from crypt base to villus base and from the crypt-villus junction to the villus tip, respectively. For scoring cell position, each crypt was divided in half and cells were numbered sequentially from crypt base to crypt-villus junction, with cell position “one” being occupied by the first cell at the base of each half crypt, as previously described. [2] Apoptosis was scored by H&E staining based on the presence of one or more pyknotic bodies at a given cell position and confirmed by immunoflorescence for cleaved caspase 3 (CC3). [34] Number of cells in G2-M phase per crypt was assessed by immunohistochemistry for phosphohistone H3 (pHH3) and counting the number of pHH3 positive cells per crypt. To directly quantify mitosis, the number of mitotic figures per crypt

was counted. Crypt density for each animal was calculated by averaging the number of crypts contained within five-500 μm lengths of mucosa. Villus height and crypt depth were measured using Axio Imager software on images captured using an Axio Imager A1 microscope and an AxioCam MRC 5 high-resolution camera (Carl Zeiss Microimaging, Inc.).

Immunostaining. For immunohistochemistry, slides were deparaffinized, rehydrated, and incubated in 3% hydrogen peroxide for 15 min at room temperature (RT) to quench endogenous peroxidase activity. Sections were treated to heat-induce epitope retrieval (Antigen Unmasking Solution cat. # H-3300, Vector Laboratories) and allowed to cool to RT. Primary antibody (rabbit anti-phospho histone H3 cat. 9701S Cell Signaling Technology) was applied to each section at 1:300 dilution and incubated for 1h at RT. Sections were then washed and incubated with biotinylated goat anti-rabbit secondary antibody for 30-60 min at RT. After washing, slides were incubated in Vectastain ABC reagent (PK-4000, Vector Laboratories) for 30 min and then developed in a DAB substrate solution. Quantification of $pHH3^{+}$ cells was performed on 25-30 crypts. Data are expressed as number of positive cells per crypt. For immunofluorescence, slides were deparaffinized, rehydrated, treated to antigen retrieval in 10mM sodium citrate (pH 6.0) with 0.05% Tween 20 for 30 min, and allowed to come to RT. Sections were washed and incubated with primary antibodies as previously reported. [3] Primary antibodies used were as follows: anti-lysozyme (sc-27958, Santa Cruz Biotechnology, 1:100 dilution), anti-mucin2 (Muc2; sc-15334, Santa Cruz Biotechnology, 1:200 dilution), and anti-active caspase 3 (cat. no. 9661, Cell Signaling Technology, 1:200 dilution). Sections were washed and incubated with corresponding fluorescently conjugated secondary antibodies. Finally, sections were mounted using Vectashield Mounting Medium with DAPI (H-1200 Vector Laboratories) and evaluated using an Axio Imager A1 microscope and an AxioCam MRC 5 high resolution camera.

293 *Statistics.* All quantitative results are presented as mean ± standard error (SE). All data were
294 subjected to one-way ANOVA with correction for multiple comparisons using the Fisher's
295 procedure. For all comparisons, a *P* value of ≤ 0.05 was considered significant.

296 **Acknowledgments**

297 This work was facilitated by services from the Cell Services and Histology Core of the Center
298 for Gastrointestinal Biology and Disease (National Institutes of Diabetes and Digestive and
299 Kidney Disease Grant P30 DK34987). Immunohistological services provided by the Histology
300 Research Core Facility in the Department of Cell Biology and Physiology at the University of
301 North Carolina, Chapel Hill NC. Work was supported by grant R01 DK100508 (C.M.D.) and
302 the Department of Surgery at the University of North Carolina at Chapel Hill.

Figure Legends

Figure1. DOXO induces apoptosis in intestinal epithelium irrespective of the presence of enteric bacteria. **A.** H&E images demonstrating mitotic bodies and immunofluorescence staining indicating the presence of active caspase 3-positive cells (green) 6h following DOXO treatment in both CONV and GF mice. Arrows indicated apoptotic cells. **B.** Quantitation of the number of apoptotic cells per crypt, for a total of 20 crypts per animal, in CONV and GF jejunal tissue from control mice and 6, 72, and 120h after DOXO treatment. * indicates values significantly different from their respective 0h controls $p \leq 0.05$. **C.** Positional analysis of apoptotic bodies in jejunal epithelium from CONV and GF mice 6h following DOXO treatment. Scale bar: 30 μm.

Figure 2. DOXO treatment does not alter crypt depth or villus height in GF mice. **A.** Micrographs of representative H&E stained sections from GF and CONV mice of control tissue and 6, 72 and 120h following DOXO treatment. **B.** Quantitation of crypt depth on 10-15 crypts/villi in CONV and GF jejunal tissue from control mice and 6, 72, and 120h after DOXO treatment. * indicates values significantly different from their respective controls $p \leq 0.05$. # indicates values significantly different within a particular time point $p \leq 0.05$. **C.** Quantitation of villus height in CONV and GF jejunal tissue from control mice and 6, 72, and 120h after DOXO treatment. Scale bar: 50 μm.

Figure 3. DOXO treatment does not impact proliferation or mitotic index in jejunal epithelium of GF mice. **A.** Micrograph showing representative staining for pHH3 on jejunal sections from GF and CONV mice. **B.** Quantitation of pHH3+ cells in CONV and GF jejunal tissue from control mice and 6, 72, and 120h after DOXO treatment. * indicates values significantly different from their respective controls $p \leq 0.05$. # indicates values significantly different within a particular time point $p \leq 0.05$. **C.** Quantitation of mitotic index in CONV and GF jejunal tissue from control mice and 6, 72, and 120h after DOXO treatment. # indicates values significantly different within a particular time point $p \leq 0.05$. ND means “not detected”. Scale bar: 50 μm.

Figure 4. DOXO treatment does not alter crypt density in jejunal mucosa of GF mice. * indicates values significantly different from their respective controls p≤0.05. # indicates values significantly different within a particular time point p≤0.05.

Figure 5. Expansion of the Paneth cell compartment and allocation of intermediate cells are not observed in GF mice following DOXO. Immunofluorescent detection of lysozyme (red), muc2 (green), and nuclei (blue) in jejunal sections from GF and CONV mice. Arrows indicate 'intermediate cells', characterized by their co-expression of lysozyme (red) and muc2 (green). Scale bar: 50 μm.

References

1. Keefe DM, Brealey J, Goland GJ, Cummins AG. Chemotherapy for cancer causes apoptosis that precedes hypoplasia in crypts of the small intestine in humans. Gut 2000; 47:632-7.

2. Dekaney CM, Gulati AS, Garrison AP, Helmrath MA, Henning SJ. Regeneration of intestinal stem/progenitor cells following doxorubicin treatment of mice. AmJPhysiol GastrointestLiver Physiol 2009; 297:G461-G70.

3. King SL, Mohiuddin JJ, Dekaney CM. Paneth cells expand from newly created and preexisting cells during repair after doxorubicin-induced damage. Am J Physiol Gastrointest Liver Physiol 2013; 305:G151-62.

4. Blaut M, Clavel T. Metabolic diversity of the intestinal microbiota: implications for health and disease. J Nutr 2007; 137:751s-5s.

5. Wu HJ, Wu E. The role of gut microbiota in immune homeostasis and autoimmunity. Gut microbes 2012; 3:4-14.

6. Artis D. Epithelial-cell recognition of commensal bacteria and maintenance of immune homeostasis in the gut. Nature reviews Immunology 2008; 8:411-20.

7. Ha CW, Lam YY, Holmes AJ. Mechanistic links between gut microbial community dynamics, microbial functions and metabolic health. World journal of gastroenterology 2014; 20:16498-517.

8. Rakoff-Nahoum S, Paglino J, Eslami-Varzaneh F, Edberg S, Medzhitov R. Recognition of Commensal Microflora by Toll-Like Receptors Is Required for Intestinal Homeostasis. Cell 2004; 118:229-41.

9. Alam M, Midtvedt T, Uribe A. Differential cell kinetics in the ileum and colon of germfree rats. Scand J Gastroenterol 1994; 29:445-51.

10. Kitajima S, Morimoto M, Sagara E, Shimizu C, Ikeda Y. Dextran sodium sulfate-induced colitis in germ-free IQI/Jic mice. Exp Anim 2001; 50:387-95.

11. Watanabe T, Higuchi K, Kobata A, Nishio H, Tanigawa T, Shiba M, Tominaga K, Fujiwara Y, Oshitani N, Asahara T, et al. Non-steroidal anti-inflammatory drug-induced small intestinal damage is Toll-like receptor 4 dependent. Gut 2008; 57:181-7.

12. Kaczmarek A, Brinkman BM, Heyndrickx L, Vandenabeele P, Krysko DV. Severity of doxorubicin-induced small intestinal mucositis is regulated by the TLR-2 and TLR-9 pathways. J Pathol 2012; 226:598-608.

13. Rigby RJ, Hunt MR, Scull BP, Simmons JG, Speck KE, Helmrath MA, Lund PK. A new animal model of post-surgical bowel inflammation and fibrosis: the effect of commensal microflora. Gut 2009.

14. Vaishnava S, Behrendt CL, Ismail AS, Eckmann L, Hooper LV. Paneth cells directly sense gut commensals and maintain homeostasis at the intestinal host-microbial interface. Proc Natl Acad Sci U S A 2008; 105:20858-63.

15. Burden DA, Osheroff N. Mechanism of action of eukaryotic topoisomerase II and drugs targeted to the enzyme. Biochim Biophys Acta 1998; 1400:139-54.

16. Gewirtz DA. A critical evaluation of the mechanisms of action proposed for the antitumor effects of the anthracycline antibiotics adriamycin and daunorubicin. Biochem Pharmacol 1999; 57:727-41.

17. Fijlstra M, Ferdous M, Koning AM, Rings EH, Harmsen HJ, Tissing WJ. Substantial decreases in the number and diversity of microbiota during chemotherapy-induced gastrointestinal mucositis in a rat model. Support Care Cancer 2015; 23:1513-22.

18. Rigottier-Gois L. Dysbiosis in inflammatory bowel diseases: the oxygen hypothesis. The ISME journal 2013; 7:1256-61.

19. Tamboli CP, Neut C, Desreumaux P, Colombel JF. Dysbiosis in inflammatory bowel disease. Gut 2004; 53:1-4.

20. Malla S, Niraula NP, Singh B, Liou K, Sohng JK. Limitations in doxorubicin production from Streptomyces peucetius. Microbiol Res 2010; 165:427-35.

21. Ballet F, Vrignaud P, Robert J, Rey C, Poupon R. Hepatic extraction, metabolism and biliary excretion of doxorubicin in the isolated perfused rat liver. Cancer chemotherapy and pharmacology 1987; 19:240-5.

22. Roberts AB, Wallace BD, Venkatesh MK, Mani S, Redinbo MR. Molecular insights into microbial beta-glucuronidase inhibition to abrogate CPT-11 toxicity. Mol Pharmacol 2013; 84:208-17.

23. Wallace BD, Roberts AB, Pollet RM, Ingle JD, Biernat KA, Pellock SJ, Venkatesh MK, Guthrie L, O'Neal SK, Robinson SJ, et al. Structure and Inhibition of Microbiome beta-Glucuronidases Essential to the Alleviation of Cancer Drug Toxicity. Chem Biol 2015; 22:1238-49.

24. Wallace BD, Wang H, Lane KT, Scott JE, Orans J, Koo JS, Venkatesh M, Jobin C, Yeh LA, Mani S, et al. Alleviating cancer drug toxicity by inhibiting a bacterial enzyme. Science 2010; 330:831-5.

25. Caballero S, Pamer EG. Microbiota-mediated inflammation and antimicrobial defense in the intestine. Annu Rev Immunol 2015; 33:227-56.

26. Salzman NH, Bevins CL. Dysbiosis--a consequence of Paneth cell dysfunction. Semin Immunol 2013; 25:334-41.

27. Nigro G, Rossi R, Commere PH, Jay P, Sansonetti PJ. The cytosolic bacterial peptidoglycan sensor Nod2 affords stem cell protection and links microbes to gut epithelial regeneration. Cell Host Microbe 2014; 15:792-8.

419 28. Stringer AM, Gibson RJ, Logan RM, Bowen JM, Yeoh AS, Laurence J, Keefe DM.
420 Irinotecan-induced mucositis is associated with changes in intestinal mucins. Cancer
421 chemotherapy and pharmacology 2009; 64:123-32.
422 29. Abreu MT, Thomas LS, Arnold ET, Lukasek K, Michelsen KS, Arditi M. TLR signaling
423 at the intestinal epithelial interface. J Endotoxin Res 2003; 9:322-30.
424 30. Niess JH, Brand S, Gu X, Landsman L, Jung S, McCormick BA, Vyas JM, Boes M,
425 Ploegh HL, Fox JG, et al. CX3CR1-mediated dendritic cell access to the intestinal lumen and
426 bacterial clearance. Science (New York, NY) 2005; 307:254-8.
427 31. Sun Z, Wang X, Wallen R, Deng X, Du X, Hallberg E, Andersson R. The influence of
428 apoptosis on intestinal barrier integrity in rats. Scandinavian Journal of Gastroenterology
429 1998; 33:415-22.
430 32. Westermann D, Lettau O, Sobirey M, Riad A, Bader M, Schultheiss HP, Tschope C.
431 Doxorubicin cardiomyopathy-induced inflammation and apoptosis are attenuated by gene
432 deletion of the kinin B1 receptor. Biol Chem 2008; 389:713-8.
433 33. Szalay CI, Erdelyi K, Kokeny G, Lajtar E, Godo M, Revesz C, Kaucsar T, Kiss N,
434 Sarkozy M, Csont T, et al. Oxidative/Nitrative Stress and Inflammation Drive Progression of
435 Doxorubicin-Induced Renal Fibrosis in Rats as Revealed by Comparing a Normal and a
436 Fibrosis-Resistant Rat Strain. PLoS One 2015; 10:e0127090.
437 34. Marshman E, Ottewell PD, Potten CS, Watson AJ. Caspase activation during
438 spontaneous and radiation-induced apoptosis in the murine intestine. Journal of Pathology
439 2001; 195:285-92.

440

Figure 1

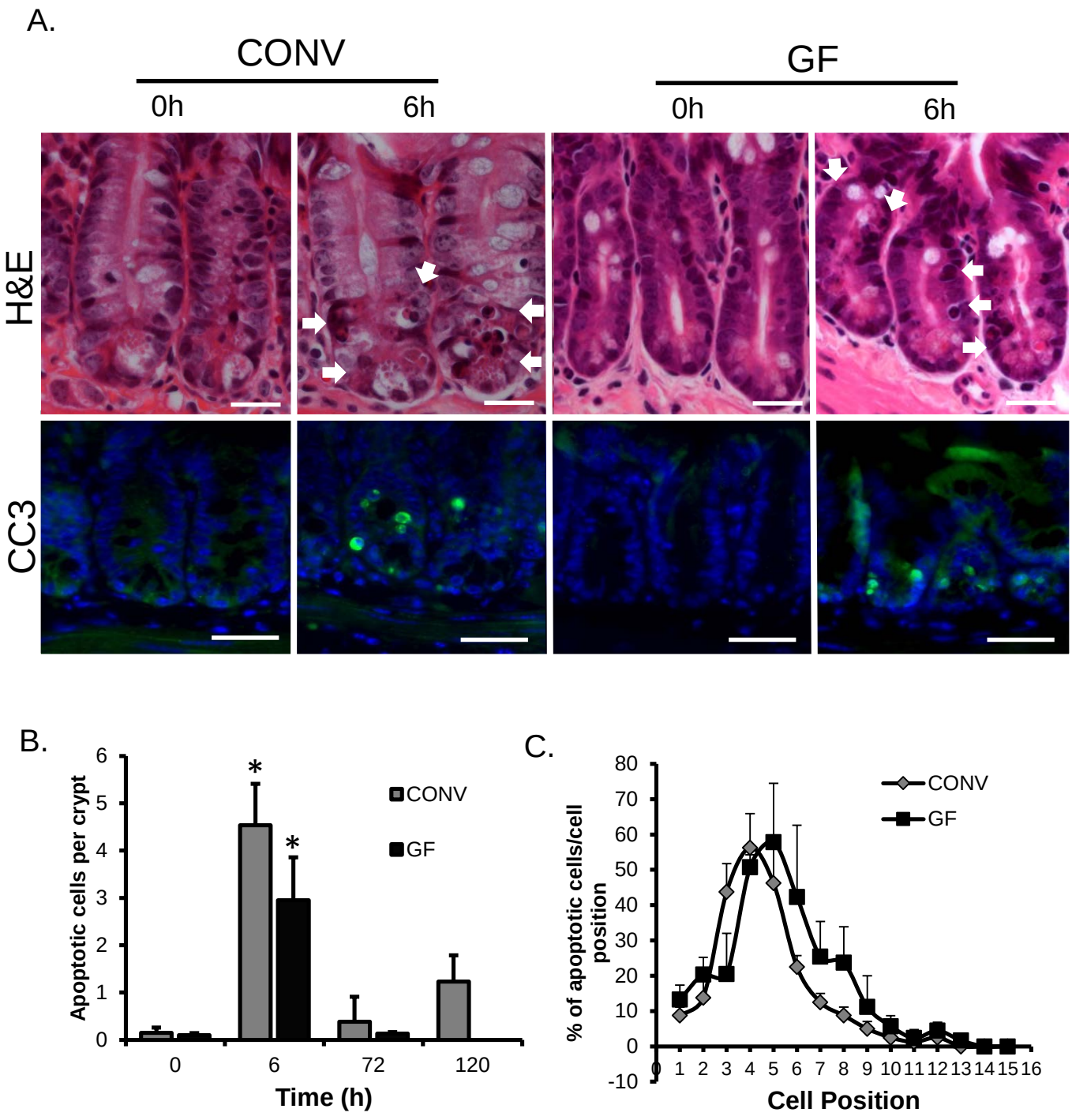
A.
CONV
GF
0h
6h
0h
6h
H&E
CC3
B.
Apoptotic cells per crypt
0
1
2
3
4
5
6
*
*
CONV
GF
0
6
72
120
Time (h)
C.
% of apoptotic cells/cell position
80
70
60
50
40
30
20
10
0
-10
CONV
GF
0 1 2 3 4 5 6 7 8 9 10 11 12 13 14 15 16
Cell Position

Figure 2

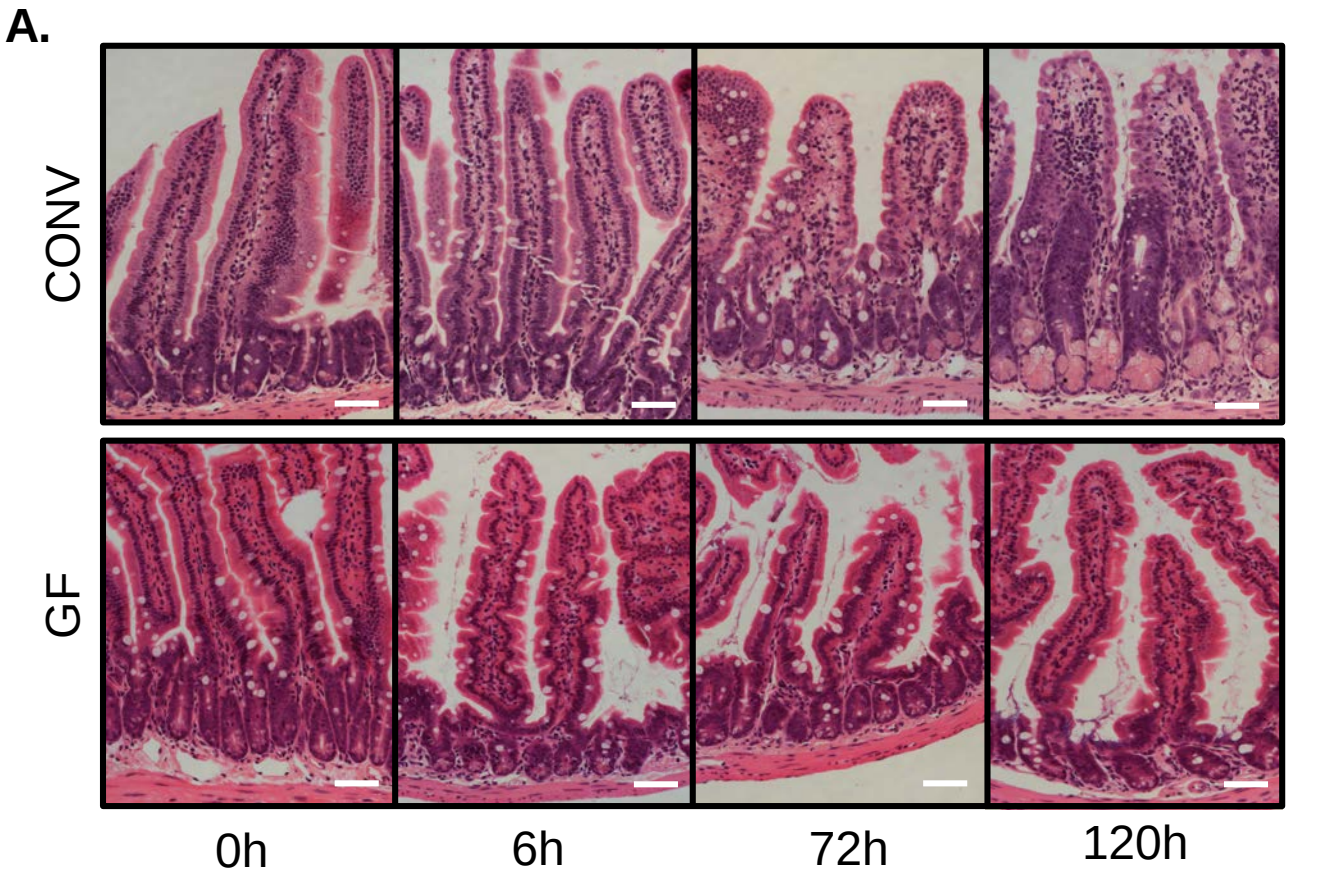
A.
CONV
GF
0h
6h
72h
120h

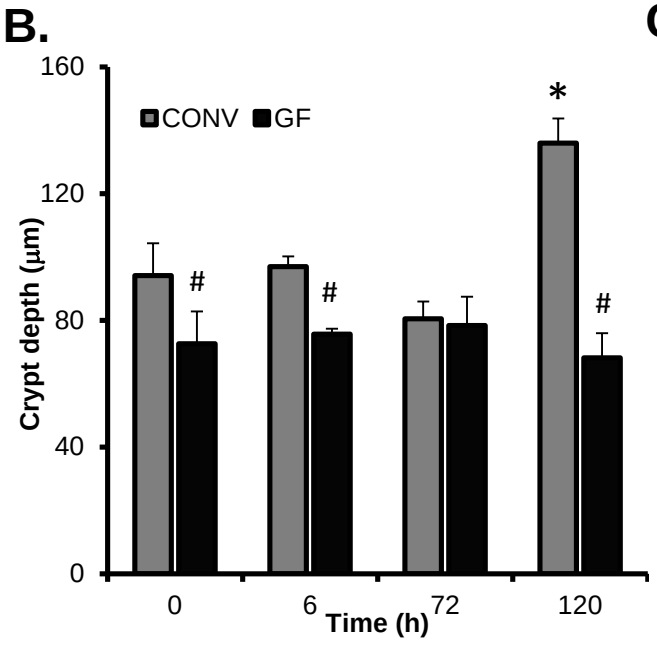
B.
CONV
GF
Crypt depth (μm)
160
120
80
40
0
#
#
#
*
0
6
72
120
Time (h)

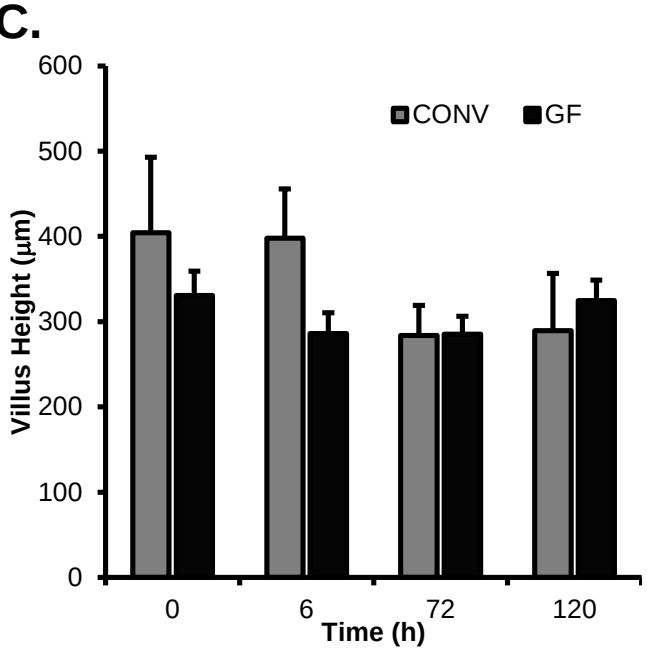
C.
CONV
GF
Villus Height (μm)
600
500
400
300
200
100
0
0
6
72
120
Time (h)

Figure 3

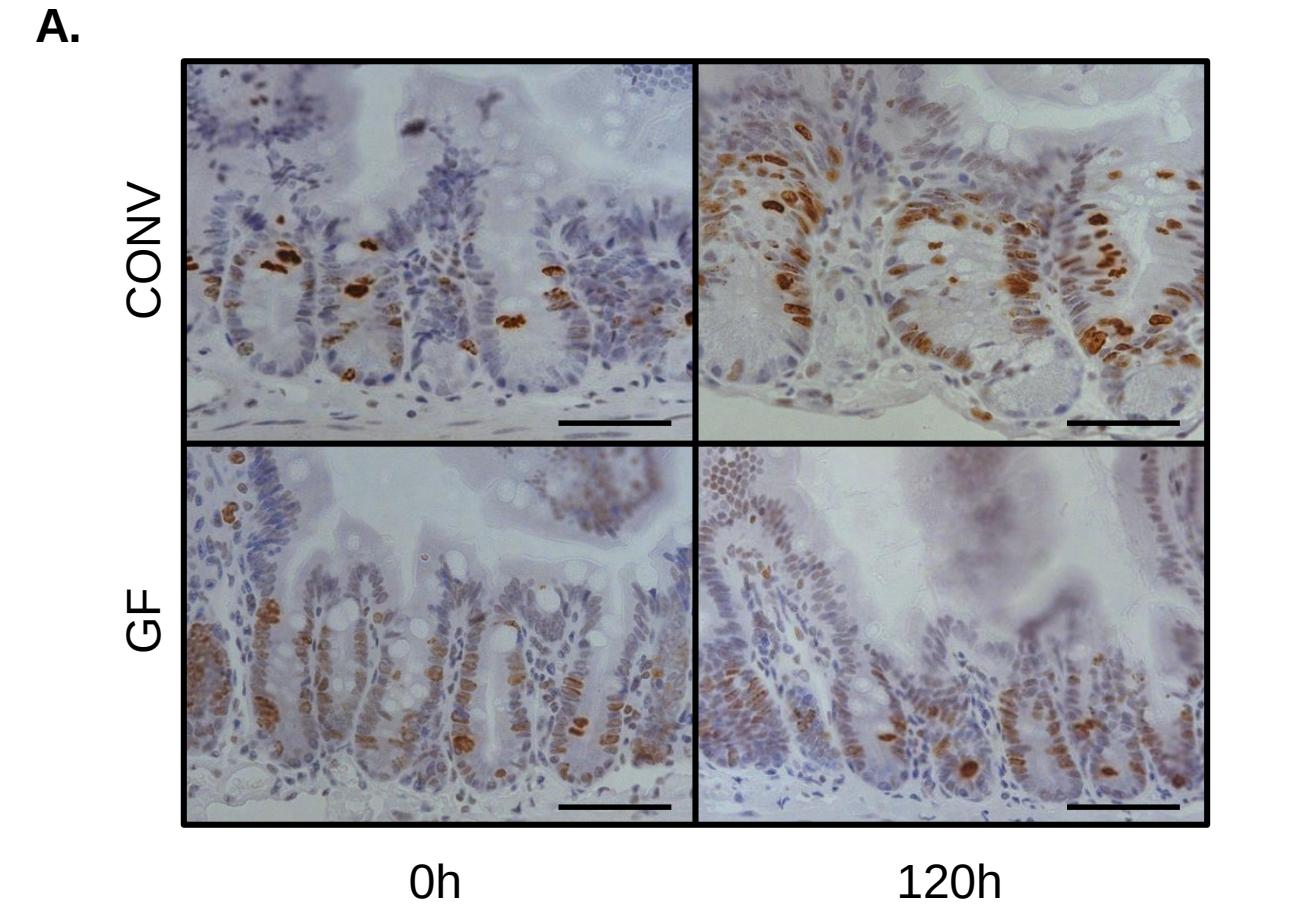
A.
CONV
GF
0h
120h
B.
Proliferative index
pH3+ cells/crypt
CONV
GF
Time (h)
C.
Mitoses
Mitoses/crypt
CONV
GF
ND
Time (h)

Figure 4

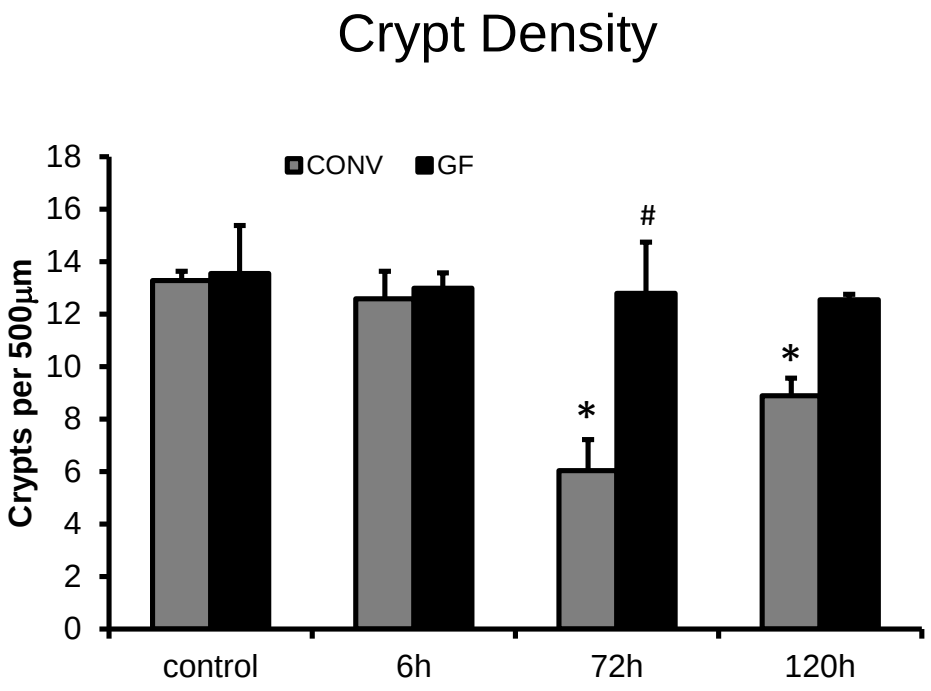
Crypt Density
CONV
GF
Crypts per 500µm
18
16
14
12
10
8
6
4
2
0
control
6h
72h
120h
*
#
*

Figure 5